A continuous approximation approach to the planar hub location-routing problem

Computers and Operations Research 100 (2018) 140–154

Contents lists available at ScienceDirect

Computers and Operations Research

journal homepage: www.elsevier.com/locate/cor

A continuous approximation approach to the planar hub location-routing problem: Modeling and solution algorithms

Nader Ghaffarinasab[a,*], Tom Van Woensel[b], Stefan Minner[c]

[a] Department of Industrial Engineering, University of Tabriz, 29th Bahman Boulevard, Tabriz 51666-14766, Iran
[b] School of Industrial Engineering & Innovation Sciences, TU Eindhoven, Eindhoven, The Netherlands
[c] TUM School of Management, Technische Universität München, Munich, Germany

ARTICLE INFO

Article history:
Received 5 October 2017
Revised 22 May 2018
Accepted 26 July 2018
Available online 27 July 2018

Keywords:
Hub location-routing problem
Transportation
Continuous approximation
Weiszfeld algorithm
Particle swarm optimization

ABSTRACT

The design of many-to-many parcel delivery networks is an important problem in freight transportation. To exploit economies of scale and provide a better service level, these networks usually have a hub-and-spoke architecture. We address a planar hub location-routing problem (HLRP) where the market demand is modeled as a uniform density function over a convex polygon service region. The continuous approximation (CA) technique is used for modeling the HLRP in such a way that it jointly decides on the location of hubs and the allocation of a service region to the hubs. The objective is to minimize the approximate total transportation cost, including local pickup and delivery costs, as well as line-haul transportation costs. Two solution algorithms are developed for the problem: an iterative Weiszfeld-type algorithm (IWA) and a particle swarm optimization (PSO) metaheuristic. The performance and solution quality of the proposed algorithms are compared with an adapted algorithm from the literature. Furthermore, extensive computational experiments are performed to study the effect of different input parameters such as the discount factor value, demand points density, and vehicle capacity on the total system cost and the final configuration of the network.

1. Introduction

Freight transportation is a vital component of the economy. It supports production, trade, and consumption activities by ensuring the efficient movement and timely availability of raw materials and finished goods. As a consequence, freight transportation accounts for a significant part of the final cost of products and represents an important component of the national expenditures of a country (Crainic and Laporte, 1997). In order to lower their costs and increase their service levels, freight carriers aim at improving their transportation and distribution network.

In freight transportation applications, as well as postal services, hub-and-spoke networks has been shown to be effective when it comes to reducing costs and delivery times, thereby increasing the service level. In such networks, the direct connections between locations in a geographic region are replaced with indirect connections facilitated by the use of hub nodes. As identified in O'Kelly and Miller (1994), such a network topology is desirable because it reduces and simplifies network construction costs, centralizes commodity handling, and allows carriers to take advantage of economies of scale through the consolidation of flows. In the case of less-than-truckload (LTL) carriers, an additional improvement is possible by serving the origin-destination (O/D) demand points along the pickup and delivery routes, rather than having to serve them separately. This can reduce the transportation costs through a more efficient use of resources (e.g. vehicles operating in the system). With these considerations in mind, the problem we study in this paper consists of two main decisions: locating hubs and generating multiple-stop routes for the non-hub points allocated to the hubs. As a result, we get the combined hub location-routing problem (HLRP). An example of the HLRP is illustrated in Fig. 1. The triangles and circles show the installed hubs and non-hub nodes, respectively. The thick lines represent the inter-hub connections (backbone links), whereas the thin lines show the local tours (access links).

Hub location, market allocation, and vehicle routing decisions belong to different levels of the decision making process and are typically treated separately in the literature. However, since strategic location and allocation decisions have a big impact on shipment costs, not taking the related routing costs into consideration in the strategic planning phase can lead to sub-optimality (Shen and Qi, 2007). Nevertheless, the detailed data on the

* Corresponding author.
E-mail addresses: ngnasab@tabrizu.ac.ir (N. Ghaffarinasab), t.v.woensel@tue.nl (T. Van Woensel), stefan.minner@tum.de (S. Minner).

https://doi.org/10.1016/j.cor.2018.07.022
0305-0548/

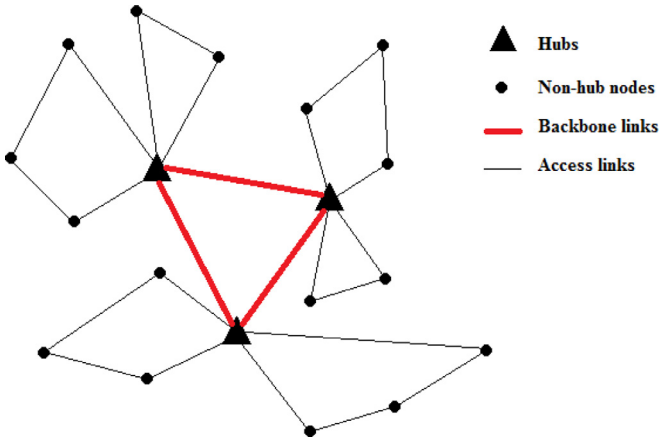

Fig. 1. HLRP solution example.

geographical locations and demand volumes of customers required as the input data for discrete network design models are seldom available when the network planner decides on the number and location of hub facilities. Continuous approximation (CA) is an alternative approach to discrete models where smooth demand density functions are used for describing the distribution system. Approximation models usually provide near optimal solutions and can address problems of larger scale and size, while discrete optimization models could provide more accurate solutions for smaller instances (Daganzo, 2005).

In this paper, we assume uniformly distributed demand points over a service region of a convex polygon shape. This assumption, which is commonly used within the CA literature, clearly makes it easier to analyze the model. However, it still provides fundamental insights into the nature of the problem and hence is a valuable complement to large, complex, and more realistic models (Erlenkotter, 1989; Geoffrion, 1976; Hall, 1986; Newell, 1973). We use the Euclidean (L_2) norm to measure the distances between points over the service area. Although some authors have argued that the L_1 distance is more realistic in urban applications as urban road networks might be better approximated by rectilinear distance, it has been shown by Von Hohenbalken and West (1984) that the market areas that were calculated by using the Euclidean distance provide fair approximations to those calculated using the rectilinear metric. We also assume that each demand point is assigned to the nearest installed hub facility based on a single allocation protocol. In the single allocation protocol, which is a common assignment scheme in many applications such as postal services, less-than-truckload (LTL) transportation, telecommunications, etc. Campbell and O'Kelly (2012), each demand node is allocated to exactly one hub.

The main contributions of this paper are threefold. First, the planar HLRP is modeled by using the CA technique for the first time in the literature that incorporates operational routing cost estimates into the strategic decisions of hub location. The problem is also formulated as a multifacility location problem. Secondly, two solution algorithms are developed: an iterative Weiszfeld-type algorithm (IWA) that exploits the characteristics of the multifacility location model and a particle swarm optimization (PSO) metaheuristic. Based on a set of experiments, it is shown that the proposed solution algorithms can obtain higher quality solutions than an adapted algorithm from the literature. Third, an extensive set of experiments is conducted to study the effect of different input factors such as the inter-hub transportation discount factor, the demand point density, and the vehicle capacity on the total system-wide costs and the number of installed hubs.

The remainder of this paper is organized as follows. The next section discusses the relevant literature. Section 3 formally defines the problem by presenting the new formulation and some definitions. The proposed solution algorithms are described in Section 4. Section 5 presents the respective experimental results and Section 6 concludes the paper and provides some directions for future research.

2. Literature review

This section presents a review of the literature for the three main research streams, namely the hub location-routing problem, CA models in location and routing problems, and the PSO algorithm.

2.1. Hub location-routing problem

Even though a large number of papers have been published on the hub location problem (HLP) and the location-routing problem (LRP), few studies have addressed the combined HLRP. A simple version of a hub location and routing problem is presented by Aykin (1995), where the hub locations and service types for the routes between the O/D pairs include three types of routes (direct, one-stop, and two-stop routes). The author proposes an iterative algorithm for solving the problem. Nagy and Salhi (1998) present a mathematical programming formulation for the HLRP where the vehicles are allowed to do the pickup and delivery on separate routes. They impose capacity and maximum distance constraints on the vehicle tours but disregard the fixed costs of using vehicles and economies of scale on the inter-hub connections. They propose a hierarchical heuristic applying the strategy of first locating and later routing embedded in a neighborhood search to solve the problem.

Zäpfel and Wasner (2002) consider the problem of planning and optimizing the hub-and-spoke transportation networks for cooperating third-party logistics providers. Mathematical models for these operational planning tasks are developed and applied to the real-case scenario of an Austrian parcel service provider.

Çetiner et al. (2010) address a hub location and routing problem under a multiple allocation setting for the Turkish postal services. They assume that the hubs are uncapacitated and vehicles have no loading constraint, but a maximum route length is imposed. They minimize both the variable transportation costs and the number of vehicles needed to achieve a given service level. They optimize the first goal by imposing an upper bound on the number of vehicles and propose an iterative hubbing and routing heuristic. Computational results using data that allow tours of no more than 450 km (one day travel time) are presented. The single allocation version of a similar problem is considered by de Camargo et al. (2013), where an upper bound is imposed on the lengths of the tours made by the vehicles in order to ensure service quality. Their objective is to minimize the sum of fixed costs for hub installation, handling costs for transferring goods at hubs, fixed costs for assigning vehicles to open hubs and distance-dependent costs for the local vehicle routes and the inter-hub transports. The authors propose a solution based on Benders decomposition embedded in a branch-and-cut framework.

Rodríguez-Martín et al. (2014) address an HLRP where exactly p hubs must be installed and thus the fixed costs for using a location as a hub are disregarded. They impose an upper bound q on the number of customerts assigned to a hub, and there is exactly one vehicle at each hub that visits the assigned customers during one multi-stop route. They propose an MIP model for the problem, along with an exact branch-and-cut algorithm. Rieck et al. (2014) consider a generalized HLRP with multiple products and the possibility of direct shipments between pickup and

delivery locations. Unlike the mail delivery applications, where each O/D pair constitutes a unique product, they assume that each O/D pair represents more than one product. There are several different products, each produced at one or several locations and demanded at one or several other locations. A homogeneous fleet of vehicles services three different types of routes: multi-stop pickup routes, direct inter-hub routes, and multi-stop delivery routes. The authors present an MIP model and devise a multi-start fix-and-optimize procedure (FOP), as well as a genetic algorithm (GA) for solving the problem.

2.2. CA models in location and routing problems

So far, not many works on the application of CA models to the hub location problem have been presented. Daganzo (1987) addresses a many-to-many distribution problem where the transportation and inventory costs are modeled by using the CA. The author assumes that the underlying network is a square grid and distances are measured by using the L_1 metric. He proposes analytical expressions for the optimal number of terminals but does not address the location problem for the terminals. Campbell (1990a,b) considers the problem of routing freight shipments via consolidation terminals (hubs) in a many-to-many logistics network and develops CA models with the aim of determining the optimal location of terminals when the costs for the consolidated inter-hub transportation are discounted. The author assumes direct shipments between origins/destinations and hubs, as well as between pairs of hubs, where the distances are measured by using the L_1 norm.

Suzuki and Drezner (1997) propose two models for the airline hub location problem in an Euclidean space. The first model assumes that all O/D traffic is routed via two hubs (the hubs located closest to the corresponding origin and destination, respectively), whereas in the second model, the flows are routed via a single hub. The problems are analyzed for the case where two hubs are selected in a square. They also analyze a three-hub case for the first model. Campbell (2013) extends Campbell (1990a) by imposing limits on the maximum travel distance via the hub network for each O/D pair. He considers a transportation carrier that serves a fixed geographic region where demand is modeled as a continuous distribution and develops analytical expressions for the optimal number of hubs, hub locations, and transportation costs.

Carlsson and Jia (2013) consider the problem of optimal hub network design in a continuous Euclidean space where the demand points are distributed uniformly over a service region. Their objective is to determine the optimal number of hub nodes and their locations. They consider seven different backbone network topologies for connecting the hub nodes, but the service at the access level is based on direct shipments. The authors describe the asymptotically optimal configurations that minimize the total network costs under the condition that the values of different input parameters become very large or very small compared to each other. They also give an approximation algorithm that solves their problem on a convex planar region for all possible values of the relevant input parameters.

Saberi and Mahmassani (2013) present CA models for airline hub location and optimal market problems where a single hub has to be located and the O/D traffic can be routed via no more that one hub. They also study the impact of a competitive airline network structure with regard to the hub location. Cachon (2014) considers a special case of the problem studied in Carlsson and Jia (2013), where the goal is to minimize the total amount of carbon emissions produced by a supply network of retail stores and the customers they serve. Pulido et al. (2015) propose a CA model for locating warehouses and designing physical distribution strategies in a one-to-many logistics network where limits on the delivery times are considered. They also study and analyze the logistics network of a Chilean firm that is active in the home delivery of a range of different products. Xie and Ouyang (2015) study the optimal layout of transshipment facilities on an infinite homogeneous Euclidean plane. They minimize the total cost that results from the facility set-up and the access and backbone transportation costs. The backbone network is assumed to be a multi-stop tour that serves the transshipment facilities from a central depot and using a vehicle of infinite capacity. Moreover, facilities serve the customers within corresponding service regions and using direct shipments. They consider both the L_2 and L_1 distance measures and provide tight upper and lower bounds on the total system cost.

The CA technique has also been used for modeling the routing costs in the traveling salesman problem (TSP), the vehicle routing problem (VRP), etc. Distance approximations for multi-stop vehicle routes play a key role in these problems. Beardwood et al. (1959) develop an analytical expression to estimate the distance covered by a traveling salesman in an area with a uniform density of destinations. Distance approximations for multiple stop routes are developed by Christofides and Eilon (1969), Eilon et al. (1971), and Daganzo (1984a, 1984b, 2005). Langevin et al. (1996) present a detailed review of applications of the CA modeling framework in freight distribution up to 1996. More recently, Francis and Smilowitz (2006) present a continuous approximation model for the periodic vehicle routing problem with service choice (PVRP-SC) where the visit frequency to nodes is a decision variable. The authors present a CA model to facilitate strategic and tactical planning of periodic distribution systems and evaluate the value of service choice.

Smilowitz and Daganzo (2007) use the CA technique for the design of integrated package distribution systems. They introduce design strategies and cost modeling techniques for multiple mode, multiple service level package delivery networks where service levels are defined by guaranteed delivery times. The authors consider key cost components such as facility charges and vehicle repositioning, transportation and inventory costs. They show that the problem can be reduced to a series of easily solvable subproblems. Jabali et al. (2012) address the fleet composition problem, which is a variant of the vehicle routing problem where the CA is used for assessing the routing costs. In their problem, the fleet size and mix are decision variables. The service region is assumed to be of a circular shape and partitioned into zones with each zone being serviced by a single vehicle. They develop a mixed integer nonlinear programming formulation followed by computationally efficient upper and lower bounding procedures.

2.3. Particle swarm optimization

Particle swarm optimization (PSO) is a population-based metaheuristic that was originally developed by Kennedy and Eberhart (1995). Inspired by the flocking (motion) of birds, PSO uses the concepts of communication and collaboration in a population of simple search agents (called particles) for solving various optimization problems. The standard PSO algorithm has undergone several refinements that finally enable to solve a large variety of discrete and continuous optimization problems (Banks et al., 2007; 2008). As a result, the PSO has successfully been used for solving a wide range of optimization problems in numerous fields (Ai and Kachitvichyanukul, 2009; Liu et al., 2012; Marinakis and Marinaki, 2010; Pedrycz et al., 2009; Sevkli and Guner, 2006; Sha and Hsu, 2008; Yang et al., 2013; Zhao et al., 2014). However, solution algorithms based on PSO for solving the hub location problems are scarce in the literature. Yang et al. (2013) solve a fuzzy p-hub center problem by using an improved hybrid PSO algorithm and combining PSO with genetic operators and local search (LS) to update and improve particles for the subproblems. They compare their hy-

brid PSO algorithm with two other solution methods, genetic algorithm (GA) and PSO without LS components, and show that the improved hybrid PSO algorithm achieves a better performance in terms of runtime and solution quality. Bailey et al. (2013) propose a PSO algorithm for the uncapacitated single allocation hub location problem (USAHLP). An empirical study that uses well-known benchmark problems from the Civil Aeronautics Board (CAB) and from the Australian Post (AP) data sets is conducted and it is shown that the proposed PSO matches or outperforms the solution quality of the best known methods for the USAHLP.

3. Model formulation

In this section, we first present the problem assumptions and then formulate the problem as a nonlinear model by using the theory of CA. The model is then reformulated as a multifacility location problem so that it can be solved by an iterative heuristic.

Consider a service region $\mathcal{A} \subset \mathbb{R}^2$ with a convex polygon shape over which a large number of clients (origins and/or destinations) are distributed. We represent the density of customers (measured in the number of clients per unit area) by a uniform continuous spatial density function $\delta(\mathbf{x}) = \delta, \mathbf{x} \in \mathcal{A}$. Assume that N is the total number of clients within the service region $\mathcal{A}$. Let the origin-destination (O/D) flow density be described as function $\lambda(\mathbf{x}, \mathbf{y})$, which gives the average number of items per time unit that need to be transported from a region of a unit area around $\mathbf{x}$ to a region of a unit area around $\mathbf{y}$. For the sake of simplicity, we assume that the average value of temporal flow between any O/D pair is one unit item, i.e., $\lambda(\mathbf{x}, \mathbf{y}) = 1$.

Collected at point $\mathbf{x}$ and delivered to point $\mathbf{y}$ by means of local pickup/delivery tours, every O/D flow is transferred through either one or two installed hubs. The vehicle fleet is assumed to be homogeneous with a capacity of C unit items. In other words, C can be interpreted as the number of stops per tour made by the vehicles. We assume that the demands are realized at different times during the planning horizon. Hence, the vehicles pick up/deliver one unit item whenever they arrive at a customer. In other words, the pickups and deliveries from/to a customer are done one at a time and on separate tours as they happen at different times. It is further assumed that the hub facilities to be installed are identical and hence have the same installation costs. Moreover, we assume that there is a limitation on the capital budget to be spent on setting up the hub facilities. Therefore, the number of hubs to be installed is exogenously determined as p hubs.

The strategic decisions to be made in the planar HLRP are location and allocation decisions. As soon as these decisions are made, the operational decisions regarding the routing of flows between O/D pairs are straightforward. The allocation of clients to hubs is based on the Euclidean distance between clients and hubs. Each hub i with location coordinates X_i serves the clients within the area closest to the respective hub. Hence, Voronoi diagrams (Aurenhammer, 1991) are used for determining the allocation decisions for a given set of located hubs. The Voronoi partition corresponding to the hub located at X_i, denoted by $\mathcal{V}_i$, is the set of all points in the service region to which the hub located at X_i is closest. For location-allocation problems with Euclidean distances, these allocation decisions are determined according to the following set definition:

$$\mathcal{V}_i = \{Y \in \mathcal{A} \mid \|Y - X_i\| \leq \|Y - X_j\|, \forall j \neq i\} \tag{1}$$

where, for every $\mathbf{x} = (x_1, x_2) \in \mathbb{R}^2$, $\|\mathbf{x}\|$ denotes the Euclidean norm, i.e., $\|\mathbf{x}\| = \sqrt{x_1^2 + x_2^2}$. Note that the service region of each hub X_i or its Voronoi partition ($\mathcal{V}_i$) is a polygon where the local deliveries in the form of vehicle routes are performed. Fig. 2 illustrates the Voronoi partitioning of a rectangular service region given the positions of 10 hubs located within it. Let W_{ij} denote the magnitude

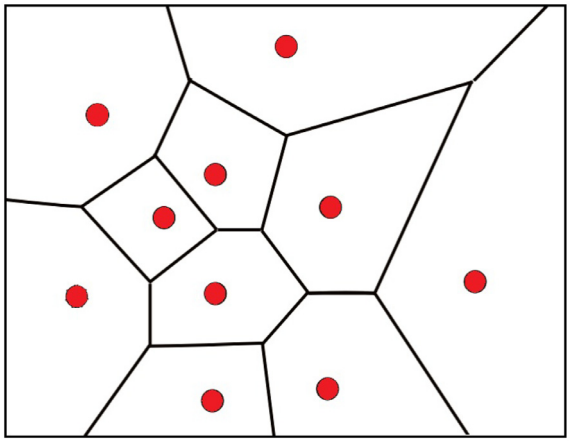

Fig. 2. Voronoi partition of a rectangular service region for a fixed set of hubs.

of the commodity flow from hub i to hub j. In other words, W_{ij} is the value of the total flow from sub-region (Voronoi cell) $\mathcal{V}_i$ to sub-region $\mathcal{V}_j$ and is calculated as:

$$W_{ij} = \lambda(\delta A_i)(\delta A_j) = \delta^2 A_i A_j \tag{2}$$

with A_i and A_j representing the areas of sub-regions $\mathcal{V}_i$ and $\mathcal{V}_j$ (in square kilometers), respectively. Note that we allow flows from nodes within a sub-region to nodes in the same sub-region. Similar to classical hub location problems, the total transportation cost in HLRP has two main components: access network cost (ANC) and backbone network cost (BNC). The former corresponds to the pickup and delivery from and to customers by means of vehicle routes within each Voronoi partition, whereas the latter corresponds to the transportation costs between hubs that are discounted by a constant factor ($0 \leq \alpha \leq 1$), which reflects the economies of scale as a result of larger flow volumes and due to the use of more efficient and/or faster means of transportation on inter-hub connections.

Since we assume that the number of hubs is an exogenous decision and that the hub establishment costs are uniform, we can ignore the costs of installing hubs in the objective function. Consequently, the continuous approximation model for the hub location-routing problem (CAHLRP) can be formulated as follows:

(**CAHLRP**)

$$\min \sum_{i=1}^{p} \sum_{j=1}^{p} \alpha W_{ij} \|X_i - X_j\|/C + 2N \sum_{i=1}^{p} VRP(\mathcal{V}_i, X_i) \tag{3}$$

$$\text{s.t.: } X_i \in \mathcal{A} \qquad i = 1, 2, \ldots, p \tag{4}$$

The first term in the objective function (3) calculates the backbone network cost (BNC), whereas the second term represents the access network cost (ANC). Both the ANC and BNC in the above formula are calculated as vehicle-kilometers. However, without loss of generality, we assume that each vehicle-kilometer of transportation costs one unit of currency (e.g., one dollar, etc.). Therefore, we can also interpret the ANC and BNC as monetary (financial) costs. The term $VRP(\mathcal{V}_i, X_i)$ denotes the cost of pickup and delivery within the Voronoi partition $\mathcal{V}_i$ from a depot located at point X_i. Note that since each customer sends and receives one unit of flow to all other customers, $VRP(\mathcal{V}_i, X_i)$ is multiplied by $2N$ in the second term of the objective function (3). Given the exact location of customers in the service region, $VRP(\mathcal{V}_i, X_i)$ can be calculated by solving the vehicle routing problem (Laporte, 1992). However, since the exact data regarding the location of future customers is seldom available in the strategic network design phase, CA is used for estimating the optimal routing costs and for utilizing

them in the decision making process about the location of hubs. Daganzo (1984a) shows that the VRP distance $VRP(\mathcal{V}_i, X_i)$ can be approximated by the following formula:

$$VRP(\mathcal{V}_i, X_i) = 2\bar{\rho}(\mathcal{V}_i, X_i)N_i/C + 0.57\sqrt{A_i N_i} \tag{5}$$

where N_i is the number of customers within the sub-region $\mathcal{V}_i$. Also, $\bar{\rho}(\mathcal{V}_i, X_i)$ denotes the average distance between the hub X_i and the customers distributed over the region $\mathcal{V}_i$ which is calculated as:

$$\bar{\rho}(\mathcal{V}_i, X_i) = \frac{\iint_{\mathcal{V}_i} \|Y - X_i\| \mathrm{d}A}{\iint_{\mathcal{V}_i} \mathrm{d}A} \tag{6}$$

A closed-form expression for $\bar{\rho}(\mathcal{V}_i, X_i)$ in which $\mathcal{V}_i$ is a convex polygon is derived in Appendix A. The first term in Eq. (5) can be interpreted as the line-haul distance between the depot and the customers, while the second term reflects the local distance between customers. The coefficients of this formula are derived by assuming $C > 6$ and $N_i > 4C^2$ (Daganzo, 1984a), which is usually true in the context of city logistics.

Note that although the model (3) and (4) is based on the assumption of equal capacities for the vehicles on backbone and access networks, it can also be used for the case of different capacities by modifying only the value of the discount factor (α). To this end, let C_B denote the capacity of the vehicles used on the backbone network, which is assumed to be γ times (usually, $\gamma > 1$) the capacity of the vehicles used on the access network (i.e., $C_B = \gamma C$). Also, assume that each vehicle-kilometer of the vehicles used on the backbone network costs b units of currency. Based on these assumptions, the objective function (3) can now be rewritten as:

$$\min \sum_{i=1}^{p}\sum_{j=1}^{p} \alpha\left(\frac{b}{\gamma}\right) W_{ij}\|X_i - X_j\|/C + 2N\sum_{i=1}^{p} VRP(\mathcal{V}_i, X_i) \tag{7}$$

As can be seen from (7), the effect of using different vehicles on the access and backbone networks can easily be captured by using a modified value for the discount factor parameter as $\alpha' = \alpha(b/\gamma)$.

In the remainder of this section, we formulate the CAHLRP as a multifacility location problem. The multifacility location problem, as defined in Francis et al. (1992), locates a fixed number of new facilities in an area where some existing (old) facilities already exist. The objective is to minimize the total cost, which is a weighted sum of the distance between each pair of new facilities and each pair constituted by an existing and a new facility. Using a new set of notations, it is not difficult to show that the model (3)–(4) can be reformulated:

(**CAHLRP-MFL**)

$$\min \sum_{1\le i<j\le p} (V_{ij} + V_{ji})\|X_i - X_j\| + \sum_{i=1}^{p} U_i \bar{\rho}(\mathcal{V}_i^k, X_i^k) + D \tag{8}$$

$$\text{s.t.: } X_i \in \mathcal{A} \qquad i = 1, 2, \ldots, p \tag{9}$$

where $V_{ij} = \alpha W_{ij}/C$, $U_i = 2N \times 2N_i/C$, and $D = 2N \times 0.57A\sqrt{\delta}$.

The model (8)–(9) is a multifacility location problem where X_j $(j = 1, \ldots, p)$ represent the location of new facilities and the customers within the sub-regions $\mathcal{V}_i$ $(i = 1, \ldots, p)$ can be seen as the locations of existing facilities. In other words, the first term in the objective function (8) calculates the cost of transportation between new facilities while the second term represents the transportation cost between existing and new facilities. Note that, since the exact locations of the customers included within each sub-region $\mathcal{V}_i$ $(i = 1, \ldots, p)$ is not known, we use the average distance $\bar{\rho}(\mathcal{V}_i^k, X_i^k)$ for all of them.

It is known that the multifacility location problem can be solved by a modified version of the well-known iterative Weiszfeld algorithm (Weiszfeld, 1973), which was originally developed for the single-facility Euclidean location problem and later extended by Miehle (1958) for the multifacility location problem (Radó, 1988).

4. Solution algorithms

In this section, we propose two solution algorithms for the CAHLRP. The first algorithm is a Weiszfelt-type algorithm (IWA), that is frequently used in the literature for solving multifacility location problems. The second solution algorithm is based on a particle swarm optimization (PSO) metaheuristic algorithm, as often successfully applied for a wide range of continuous and discrete optimization problems.

4.1. Iterative Weiszfeld-type algorithm

We propose the IWA for solving the multifacility model CAHLRP-MFL in an iterative manner. Since the exact locations of the demand points within each sub-region $\mathcal{V}_i$ $(i = 1, \ldots, p)$ are not known, we represent all the demand points within the sub-region $\mathcal{V}_i$ by the geometric median or Fermat–Weber point $FW(\mathcal{V}_i)$ of this region defined as:

$$FW(\mathcal{V}_i) = \underset{Y\in\mathcal{V}_i}{\operatorname{argmin}} \iint_{\mathcal{V}_i} \|X - Y\| \mathrm{d}A = \underset{Y\in\mathcal{V}_i}{\operatorname{argmin}}\ \bar{\rho}(\mathcal{V}_i, Y) \tag{10}$$

Based on the above explanations, it is now possible to adapt the Weiszfelt's algorithm for our own problem. Having generated an initial solution, a new solution based on the solution from the previous iteration is generated at each iteration. The following equations are used for this purpose:

$$X_i^{k+1} = \frac{\sum_{j\neq i} \frac{(V_{ij}^k + V_{ji}^k)}{\|X_i^k - X_j^k\|} X_j^k + \frac{U_i}{\bar{\rho}(\mathcal{V}_i^k, X_i^k)} FW(\mathcal{V}_i^k)}{\sum_{j\neq i} \frac{(V_{ij}^k + V_{ji}^k)}{\|X_i^k - X_j^k\|} + \frac{U_i}{\bar{\rho}(\mathcal{V}_i^k, X_i^k)}}, \qquad i = 1, 2, \ldots, p \tag{11}$$

The proposed IWA algorithm works as follows. At the beginning, the counter k representing the main algorithm iterations is set to 0. An initial solution X_i^0 $(i = 1, 2, \ldots, p)$ is first generated as a collection of p points randomly generated over the service region. At each iteration k, based on the current solution X_i^k $(i = 1, 2, \ldots, p)$ and the values evaluated for W_{ij}^k, $\bar{\rho}(\mathcal{V}_i^k, X_i^k)$ and $FW(\mathcal{V}_i^k)$, $(i, j = 1, 2, \ldots, p)$, the next solution X_i^{k+1} $(i = 1, 2, \ldots, p)$ is generated using Eq. (11) and the new Voronoi partitions are determined for each installed hub. Also, the objective function value is then evaluated using Eq. (8). We use another counter denoted by t that counts the number of iterations for which all hubs stay within a distance of ν from their previous positions. When the counter t is larger than the pre-specified threshold value N_{nonimp}, the algorithm terminates. The pseudo-code for the IWA is illustrated in Algorithm 1.

4.2. PSO algorithm

The PSO (Kennedy and Eberhart, 1995) is a population-based evolutionary optimization algorithm inspired by social interaction and communication in bird flocking or fish schooling. Due to its successful performance and rather easy implementation, there has recently been a high increase in the use of PSO for solving different optimization problems. A population of N_{pop} candidate solutions, called particles, collaborate simultaneously and move around the feasible solution space in a systematic way in order to reach the best positions in that space. Each solution s consists of a position vector $\vec{x}^s$ and a velocity vector $\vec{v}^s$. Given the particle's previous best position $\vec{p}_b^s$ and the previous best position attained by any particle of the swarm $\vec{g}_b$, the velocity vector for particle s is obtained by:

$$\vec{v}_t^s = \omega\vec{v}_t^s + \varphi_1 r_1(\vec{p}_b^s - \vec{x}_{t-1}^s) + \varphi_2 r_2(\vec{g}_b - \vec{x}_{t-1}^s) \tag{12}$$

Algorithm 1 Pseudo-code for the iterative Weiszfeld-type algorithm $(\mathcal{A}, p, N_{nonimp}, \nu, \epsilon)$.

Define and initialize the model parameters and variables
$t \leftarrow 0$
$k \leftarrow 0$
Generate an initial set of p hubs X_i^0 $(i = 1, \ldots, p)$ over the service region $\mathcal{A}$
Construct the Voronoi partitions $\mathcal{V}_i^0$ $(i = 1, \ldots, p)$ based on the installed hubs within $\mathcal{A}$
while $t \leq N_{nonimp}$ **do**
  Evaluate W_{ij}^k, $i, j = 1, 2, \ldots, p$ using (2)
  Evaluate $\bar{\rho}(\mathcal{V}_i^k, X_i^k)$, $i = 1, 2, \ldots, p$ using (A.3)
  Evaluate the objective function $f(X^k)$ using (3)
  Minimize (10) to obtain the Fermat-Weber point of Voronoi cell i, $FW(\mathcal{V}_i^k)$, $i = 1, 2, \ldots, p$
  Compute X_i^{k+1}, $i = 1, 2, \ldots, p$ using (11)
  if $\|X_i^{k+1} - X_i^k\| \geq \nu$ for any i $(i = 1, 2, \ldots, p)$ **then**
    $t \leftarrow 0$
    $k \leftarrow k + 1$
  else
    $k \leftarrow k + 1$
    $t \leftarrow t + 1$
  end if
end while
return X^k, $f(X^k)$.

Algorithm 2 Pseudo-code for the PSO algorithm $(\mathcal{A}, p, N_{pop}, w, \varphi_1, \varphi_2, I_{max})$.

Define and initialize the model parameters and variables
$t \leftarrow 0$
Generate an initial population of N_{pop} particles $\vec{x}_0^s$ $(s = 1, \ldots, N_{pop})$ over the service region $\mathcal{A}$
while $t \leq I_{max}$ **do**
  for s = 1 to N_{pop} **do**
    Evaluate the particles' fitness $f(\vec{x}_t^s)$ using (3)
    Update particle's velocity $\vec{v}_t^s$ using (12)
    Update particle's position $\vec{x}_t^s$ using (13)
    Keep the particle within the boundaries of the service region $(\vec{x}_t^s \in \mathcal{A})$
    if $f(\vec{x}_t^s) < f(\vec{p}_b^s)$ **then**
      $\vec{p}_b^s \leftarrow \vec{x}_t^s$
    end if
    if $f(\vec{x}_t^s) < f(\vec{g}_b)$ **then**
      $\vec{g}_b \leftarrow \vec{x}_t^s$
    end if
  end for
  $t \leftarrow t + 1$
end while
return $\vec{g}_b$, $f(\vec{g}_b)$.

where ω is the inertia weight that controls the momentum of the particle and φ_1 and φ_2 are the weights that represent the attraction toward positions $\vec{p}_b^s$ and $\vec{g}_b$, respectively. r_1 and r_2 are random numbers and are uniformly distributed in the interval [0,1]. Having obtained the velocity vector for the particle s, its position vector is updated by:

$$\vec{x}_t^s = \vec{x}_{t-1}^s + \vec{v}_t^s \tag{13}$$

Note that, for each particle s, the corresponding position vector is not allowed to go beyond the boundaries of the solution space (service region) during the iterations of the algorithm.

In our implementation, each particle is represented by a $2 \times p$ matrix that shows the x and y coordinates of the p hubs. An initial population is generated as a set of N_{pop} randomly scattered points within the service area $\mathcal{A}$. The velocity and position vectors of the particles are updated throughout the algorithm iterations based on (12) and (13), respectively. The algorithm terminates as soon as a threshold for the number of iterations (I_{max}) is reached. The pseudo-code for the proposed PSO is illustrated in Algorithm 2.

5. Computational experiments

In this section, we describe the computational experiments we conducted to evaluate the efficiency of the proposed algorithms and to investigate the effect of different input parameters on the solution characteristics of the proposed model. The solution algorithms are coded in MATLAB R2014a and all the experiments were run on a computer with Intel(R) Core(TM) i3-3220 CPU of 3.30 GHz and 16GB of RAM, using the Microsoft Windows 7 operating system. Voronoi partitioning of the service region based on the location of hubs is performed using the open-source Multi-Parametric Toolbox 3.0 (MPT3), a MATLAB-based toolbox for parametric optimization, computational geometry and model predictive control (Herceg et al., 2013). Furthermore, the Fermat-Weber points used at every iteration of the IWA are calculated by minimizing (10) using the function "fminunc" from MATLAB Optimization Toolbox. The average distances $\bar{\rho}(\mathcal{V}_i, Y)$ in (10) are calculated by using the closed-form formula derived for this purpose in Appendix A. The base test instances are generated assuming a square service region with a side lengths of 10 km (a total area of 100 km^2), which is the dimension of many medium-sized cities world-wide. Demand points density (δ) is set to 50 per square kilometer. The capacity of vehicles (C) is assumed to be 10 units of load (maximum of 10 stops per tour). The number of hubs to be installed in this service region (p) is set to different values from the set $\{2, 3, \ldots, 10\}$. The default value for the discount factor associated with inter-hub transportation costs is $\alpha = 0.4$. However, to study the effect of variations in the values of input parameters on the quality of solutions, the above-mentioned default values are allowed to alter as $\alpha \in \{0.4, 0.6, 0.8\}$, $\delta \in \{30, 50, 70\}$, and $C \in \{7, 10, 13\}$, later in our computational experiments.

The parameters of the proposed algorithms are tuned in such a way that they produce high quality solutions within a reasonable time frame. Based on the results we obtained through a set of preliminary experiments, the best values for the parameters of the two algorithms are selected. For the IWA algorithm, the distance tolerance level ν and the threshold value N_{nonimp} were selected as 0.001 and 30, respectively. For the PSO algorithm, the population size N_{pop} was chosen as 60, whereas the total number of iterations I_{max} was set to 100. Furthermore, the inertia weight ω we selected was 0.9 and the attraction weights φ_1 and φ_2 were defined as 0.6 and 0.3, respectively.

5.1. Numerical results

A comprehensive set of computational experiments was conducted using the above mentioned test problems to show the efficiency of the proposed algorithms and the results are presented in the remainder of this section. For each problem instance, both algorithms were run for three times (as the final solution depends on the initial solution, which is generated randomly) and the best solutions obtained are reported.

Table 1 shows the results obtained by solving the CAHLRP by using the proposed solution algorithms with a discount factor value of α=0.4. The first column of this table shows the number of hubs to be opened (p). The column "TC" gives the total transportation cost (in thousand units) obtained by the algorithms as the

Table 1
Results for solving the problem with $\alpha = 0.4$.

p	IWA						PSO					
	TC	ANC	BNC	%ANC	%BNC	CPU(s)	TC	ANC	BNC	%ANC	%BNC	CPU(s)
2	36022.32	33820.21	2202.11	93.89%	6.11%	3.96	36018.86	33865.25	2153.61	94.02%	5.98%	162.42
3	31012.91	27713.39	3299.51	89.36%	10.64%	4.03	31002.91	27791.17	3211.74	89.64%	10.36%	234.11
4	27242.92	23255.27	3987.64	85.36%	14.64%	4.68	27221.31	23367.90	3853.41	85.84%	14.16%	314.01
5	25797.02	21631.22	4165.79	83.85%	16.15%	14.69	25793.28	21680.91	4112.37	84.06%	15.94%	332.18
6	24529.15	20222.01	4307.14	82.44%	17.56%	8.10	24523.66	20269.04	4254.61	82.65%	17.35%	384.53
7	23432.08	19000.68	4431.40	81.09%	18.91%	12.48	23428.25	19048.65	4379.59	81.31%	18.69%	507.08
8	22398.82	17856.75	4542.06	79.72%	20.28%	26.35	22397.38	17876.69	4520.69	79.82%	20.18%	506.81
9	21513.24	16876.44	4636.80	78.45%	21.55%	14.85	21518.27	16908.96	4609.31	78.58%	21.42%	577.66
10	21000.19	16327.90	4672.29	77.75%	22.25%	23.76	21040.59	16421.76	4618.83	78.05%	21.95%	639.91
Avg.	25883.18	21855.99	4027.19	83.55%	16.45%	12.54	25882.72	21914.48	3968.24	83.77%	16.23%	406.52

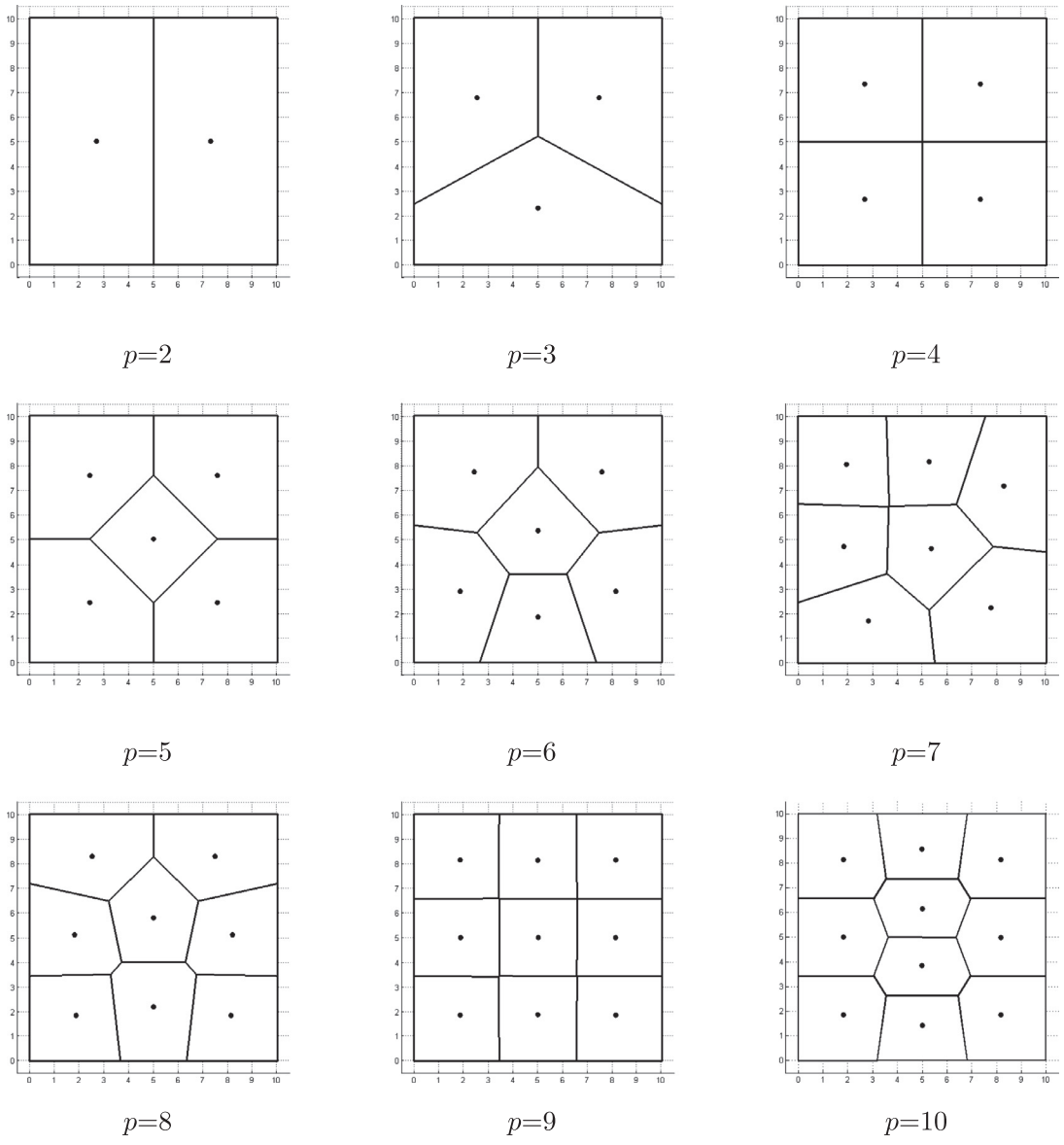

Fig. 3. Network configuration for different values of p with $\alpha = 0.4$.

value of the objective function. The access network cost (ANC) and the backbone network cost (BNC) are reported in columns "ANC" and "BNC", respectively. The next two columns, labeled as "%ANC" and "%BNC", show the values of the access and backbone network costs as percentage of the total transportation cost. The column "CPU(s)" gives the solution time (in seconds). Finally, the last row reports the average values of all the reported quantities for the two proposed algorithms.

Table 1 shows that the solutions that were obtained by the two algorithms have almost the same objective value for each instance. In most of the instances, the cost of the solution obtained by the PSO is slightly smaller than that of the IWA. However, for some in-

Table 2
Results for solving the problem with $\alpha = 0.6$.

p	IWA						PSO					
	TC	ANC	BNC	%ANC	%BNC	CPU(s)	TC	ANC	BNC	%ANC	%BNC	CPU(s)
2	37059.27	33983.19	3076.08	91.70%	8.30%	3.62	37051.84	34085.00	2966.84	91.99%	8.01%	150.67
3	32579.79	27868.15	4711.64	85.54%	14.46%	4.63	32557.83	28042.80	4515.03	86.13%	13.87%	205.12
4	29143.81	23376.40	5767.40	80.21%	19.79%	7.73	29096.07	23629.46	5466.61	81.21%	18.79%	262.95
5	27815.25	21785.80	6029.45	78.32%	21.68%	11.13	27837.06	22021.09	5815.97	79.11%	20.89%	332.64
6	26622.40	20365.96	6256.44	76.50%	23.50%	15.42	26608.02	20486.38	6121.64	76.99%	23.01%	383.20
7	25592.61	19137.41	6455.20	74.78%	25.22%	10.59	25542.77	19223.95	6318.82	75.26%	24.74%	451.88
8	24624.47	17989.07	6635.40	73.05%	26.95%	11.46	24582.14	18013.85	6568.28	73.28%	26.72%	514.49
9	23785.89	16995.82	6790.07	71.45%	28.55%	16.35	23787.03	17070.17	6716.86	71.76%	28.24%	594.27
10	23298.21	16450.55	6847.66	70.61%	29.39%	19.76	23344.05	16576.98	6767.06	71.01%	28.99%	657.04
Avg.	27835.74	21994.71	5841.04	78.02%	21.98%	11.19	27822.98	22127.74	5695.23	78.53%	21.47%	394.70

Table 3
Results for solving the problem with $\alpha = 0.8$.

p	IWA						PSO					
	TC	ANC	BNC	%ANC	%BNC	CPU(s)	TC	ANC	BNC	%ANC	%BNC	CPU(s)
2	38009.63	34217.06	3792.57	90.02%	9.98%	3.46	37997.24	34392.13	3605.11	90.51%	9.49%	152.54
3	34049.04	28091.29	5957.75	82.50%	17.50%	5.70	34011.27	28398.46	5612.81	83.50%	16.50%	207.73
4	30948.76	23550.94	7397.82	76.10%	23.90%	4.79	30865.11	24001.49	6863.62	77.76%	22.24%	265.97
5	29743.02	22007.31	7735.71	73.99%	26.01%	9.53	29720.62	22275.69	7444.93	74.95%	25.05%	331.92
6	28630.58	20571.82	8058.76	71.85%	28.15%	7.34	28603.15	20809.19	7793.96	72.75%	27.25%	387.92
7	27671.66	19330.45	8341.21	69.86%	30.14%	8.90	27692.71	19597.07	8095.64	70.77%	29.23%	460.89
8	26775.27	18175.75	8599.52	67.88%	32.12%	12.17	26755.72	18341.33	8414.38	68.55%	31.45%	527.66
9	25990.58	17169.07	8821.51	66.06%	33.94%	20.08	25989.03	17321.94	8667.09	66.65%	33.35%	597.56
10	25531.14	16627.43	8903.71	65.13%	34.87%	17.45	25511.76	16768.63	8743.12	65.73%	34.27%	649.76
Avg.	29705.52	22193.46	7512.06	73.71%	26.29%	9.94	29682.96	22433.99	7248.96	74.57%	25.43%	397.99

stances (such as $p = 9,10$), the IWA renders a better solution than the PSO. Analyzing the two components of the transportation cost, we observe that the access network cost (ANC) has a larger share in the transportation cost than the backbone network cost (BNC), which means that the local pickup and delivery via vehicle routes comes at a significantly higher cost than the consolidated line-haul transportation between hubs. Note that, as the number of hubs gets larger, the backbone network cost (BNC) increases as a result of the longer total distance between the installed hubs. Another interesting observation is that the access network cost (ANC) decreases as the number of hubs increases. This result may not seem intuitive at first sight but it is in line with the general assumption of the continuous approximation literature, where transportation costs are modeled proportional to the square of the service region size (Murat et al., 2010). More specifically, when the number of hubs increases, the service region assigned to each hub gets smaller on average. However, the average distance between an installed hub and the customers inside the corresponding service region decreases non-linearly relative to the size of the service region, which in turn results in a much smaller access network cost incurred by pickup and delivery routes.

Note that, from a solution time perspective, both algorithms solve the CAHLRP in short computational times, although the IWA is much faster than the PSO. The IWA solves the instances in less than 15 s on average, whereas the average time for the PSO is more than 400 s for the same set of problems. Comparing the solution times, one can conclude that the computational burden for calculating the Fermat-Weber points (which is only used in the IWA) is not substantial. Furthermore, the results show that the solution times for both algorithms depend on the number of hubs to be opened as a higher number of hubs needs more computational effort for partitioning the service region and calculating the average distance for each partition.

For every solution obtained by the IWA and reported in Table 1, we plotted the location of hubs in the service region along with the corresponding Voronoi partitions and depicted the resulting network configurations in Fig. 3. The solutions obtained by the PSO have similar configurations.

It can be seen from Fig. 3 that the hubs are scattered within the service region based on symmetric and uniform patterns and the resulting Voronoi partitions are of almost the same size. This is mainly due to the uniform distribution of the customers over the service region.

5.2. Studying the effect of the discount factor

The discount factor (α) plays an important role in the final configuration of the network in hub location problems. In this section, we present the results of solving our problem under different values of α. The results we obtained by solving the CAHLRP with discount factor values α=0.6 and 0.8 are reported in Tables 2 and 3, respectively.

Observe that the increase in value of the discount factor (α) results in increased values for both the ANC and the BNC and hence increased total transportation cost. It should also be noted that the share of the BNC from the TC gets larger as the value of α increases. For instance, the BNC makes up (on average) around 16%, 21%, and 26% of the TC for the cases with $\alpha = 0.4$, 0.6, and 0.8, respectively. This is due to the fact that, by setting α to a large value, the amount of discount granted on the inter-hub transportations gets smaller and hence, the corresponding cost increases.

To get a better visualization of the effect of the discount factor on the location of hubs, the final network configuration for different values of α are plotted in Fig. 4 for problems with 5 and 10 hubs. Three different values for the discount factor value are used as $\alpha \in \{0.0, 0.5, 1.0\}$. The parts we colored in red correspond to the network configuration under $\alpha = 0.0$, whereas the blue and gray parts correspond to the networks under $\alpha = 0.5$ and 1.0, respectively. The black parts are common for all the three values of α.

We can see from Fig. 4 that increasing the value of α makes the location of hubs move closer to each other at the center of the service region. This can be interpreted as a consequence of the

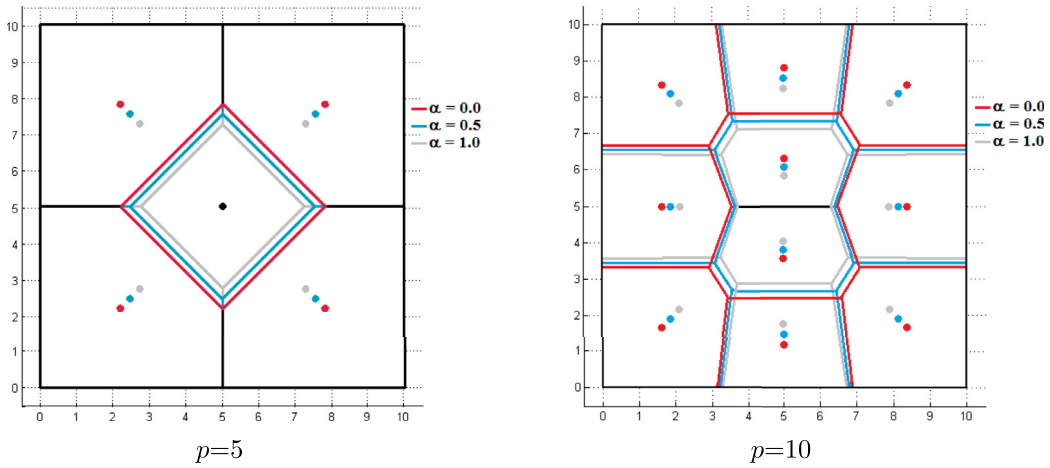

Fig. 4. Network configuration for $p = 5$ and 10 with different values of α.

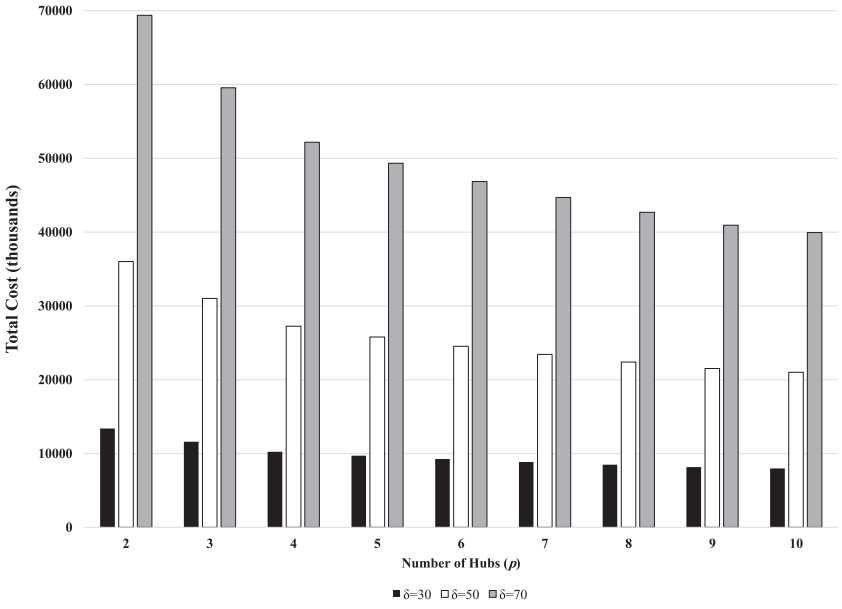

Fig. 5. Total transportation cost for different values δ with $\alpha = 0.4$ and $C = 10$.

increased inter-hub transportation cost that makes the algorithms reduce the distance between the hubs to partly diminish the effect of increased α values. However, the decrease in the BNC as a result of closer hub facilities does not compensate its increase as a result of larger α values. As a result, the BNC increases as the discount factor value gets larger. Furthermore, for larger values of α, the hubs go far from the Fermat-Weber points of corresponding Voronoi partitions, which results in slightly increased ANC compared to the case where each hub is located exactly at the Fermat-Weber point of the corresponding Voronoi partition. Therefore, a trade-off has to be done between the BNC and the ANC components of the total transportation cost.

5.3. The effect of other input parameters

In this part of our computational experiments, we study the effect of adopting alternative values for two other input parameters, namely the demand point density (δ) and the vehicle capacity (C), on the total transportation cost of the system. To this end, we first study the effect of δ by using three values for the demand point density as $\delta \in \{30, 50, 70\}$ and solve the problem by taking the default values as the input for the other parameters (i.e., $\alpha = 0.4$ and $C = 10$). Fig. 5 illustrates the total transportation cost for varying numbers of hubs under three different values of δ.

As can be seen from Fig. 5, larger values of demand point density result in substantially higher total cost as both the access and backbone network costs are increased for larger values of δ. Furthermore, as mentioned earlier, an increase in the number of installed hubs (p) results in smaller transportation cost.

We will now study the effect of the vehicle capacity (C) on the total transportation cost. Fig. 6 illustrates the total cost under three different values we selected for the vehicle capacity: $C \in \{7, 10, 13\}$ for different numbers of installed hubs by assuming that the other input parameters take their default values (i.e., $\alpha = 0.4$ and $\delta = 50$).

Observe from Fig. 6 that, as the vehicle capacity (C) increases, the total transportation cost decreases. This is because, if one uses smaller vehicles, more vehicle-kilometers are needed to transfer the O/D flows between the corresponding origins and destinations.

5.4. Evaluating the quality of the proposed solution algorithms

In order to evaluate the quality of our proposed solution algorithms, we compare the solutions obtained by our algorithms

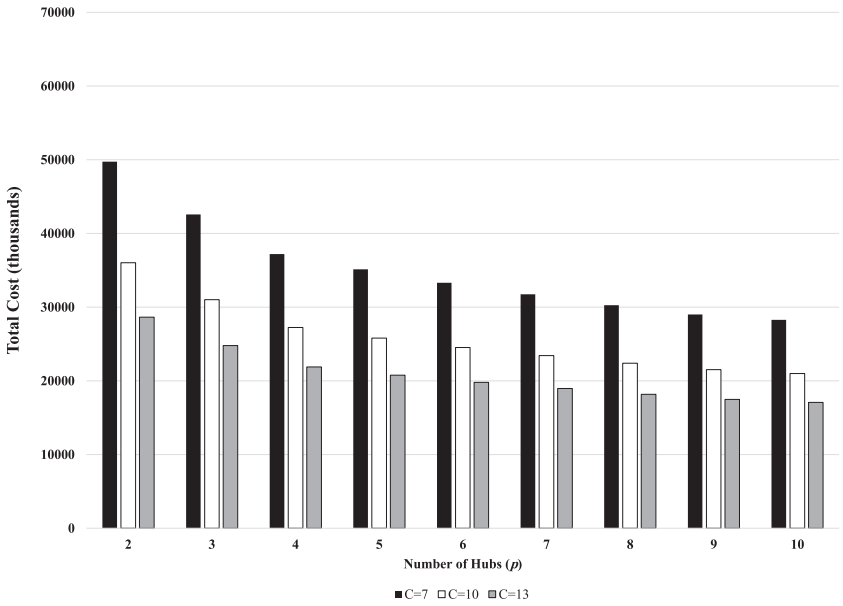

Fig. 6. Total transportation cost for different values C with $\alpha = 0.4$ and $\delta = 50$.

Table 4
Results for solving the problem by the algorithm proposed by Carlsson and Jia (2013) with $\delta = 50$ and $C = 10$.

p	$\alpha = 0.4$			$\alpha = 0.6$			$\alpha = 0.8$		
	Total Cost	Gap with		Total Cost	Gap with		Total Cost	Gap with	
	C&J	IWA	PSO	C&J	IWA	PSO	C&J	IWA	PSO
2	36192.17	0.47%	0.48%	37442.17	1.03%	1.05%	38692.17	1.80%	1.83%
3	31300.73	0.93%	0.96%	33100.76	1.60%	1.67%	34900.79	2.50%	2.62%
4	27428.16	0.68%	0.76%	29562.05	1.44%	1.60%	31695.93	2.41%	2.69%
5	26165.61	1.43%	1.44%	28375.41	2.01%	1.93%	30585.21	2.83%	2.91%
6	24741.74	0.87%	0.89%	27029.80	1.53%	1.59%	29317.87	2.40%	2.50%
7	23619.83	0.80%	0.82%	25936.05	1.34%	1.54%	28252.28	2.10%	2.02%
8	23544.25	5.11%	5.12%	25885.70	5.12%	5.30%	28227.15	5.42%	5.50%
9	22486.03	4.52%	4.50%	24844.37	4.45%	4.45%	27202.70	4.66%	4.67%
10	21446.05	2.12%	1.93%	23817.45	2.23%	2.03%	26188.84	2.58%	2.65%
Avg.	26324.95	1.88%	1.88%	28443.75	2.31%	2.35%	30562.55	2.97%	3.04%

to those obtained by the algorithm proposed by Carlsson and Jia (2013) on the instances with a square service region. For doing so, first the solution procedure presented in Carlsson and Jia (2013) is implemented to determine the location of a fixed number of hubs and the corresponding Voronoi partitions. Then the objective function values of the obtained solutions are evaluated by using (3). The results for different values of α with $\delta = 50$ and $C = 10$ are reported in Table 4. Note that, since the number of hubs in our problem is fixed, we do not need to run Algorithm 3 of Carlsson and Jia (2013) and we only run the algorithms "ApproxFW" and "RectanglePartition" to determine the location of p hubs. The total cost values obtained for different instances, as well as the gap percentage between the obtained objective function values and those of the IWA and PSO, are reported. The gap percentage values are calculated by using the following formula:

$$\text{Gap} = \frac{OF_{C\&J} - OF_{IWA(PSO)}}{OF_{IWA(PSO)}} \times 100\%$$

where $OF_{C\&J}$ represents the objective function value obtained by Carlsson and Jia's algorithm and $OF_{IWA(PSO)}$ is the objective function value obtained by the IWA (or the PSO).

The results reported in Table 4 show that both of our proposed algorithms (i.e., the IWA and PSO) outperform the algorithm proposed in Carlsson and Jia (2013) for all the tested instances. For the IWA, the average gap between the objective values under $\alpha = 0.4$, 0.6, and 0.8 are 1.88, 2.31, and 2.97 %, respectively. The corresponding gap values for the PSO are 1.88, 2.35, and 3.04 %, respectively. Therefore, it can be concluded that both the proposed algorithms perform better than an existing algorithm from the literature in terms of solution quality. An interesting observation form Table 4 is that the average gap between the Carlsson and Jia's algorithm and the proposed algorithms increases as the value of the discount factor gets larger. In other words, the solutions obtained by the Carlsson and Jia's algorithm perform much better under smaller values of the discount factor α.

Fig. 7 depicts the corresponding network configurations obtained by the Carlsson and Jia's algorithm for the tested instances. The network configurations are identical for different values of α.

The results for solving the problem using the Carlsson and Jia's algorithm as well as the proposed heuristics for different values of demand points density δ with $\alpha = 0.4$ and $C = 10$ are reported in Table 5. It can also be seen from this table that the proposed algorithms perform better than the Carlsson and Jia's algorithm for all the tested instances.

Table 6 presents the results for solving the problem using the three algorithms for different values of vehicle capacity C with $\alpha = 0.4$ and $\delta = 50$.

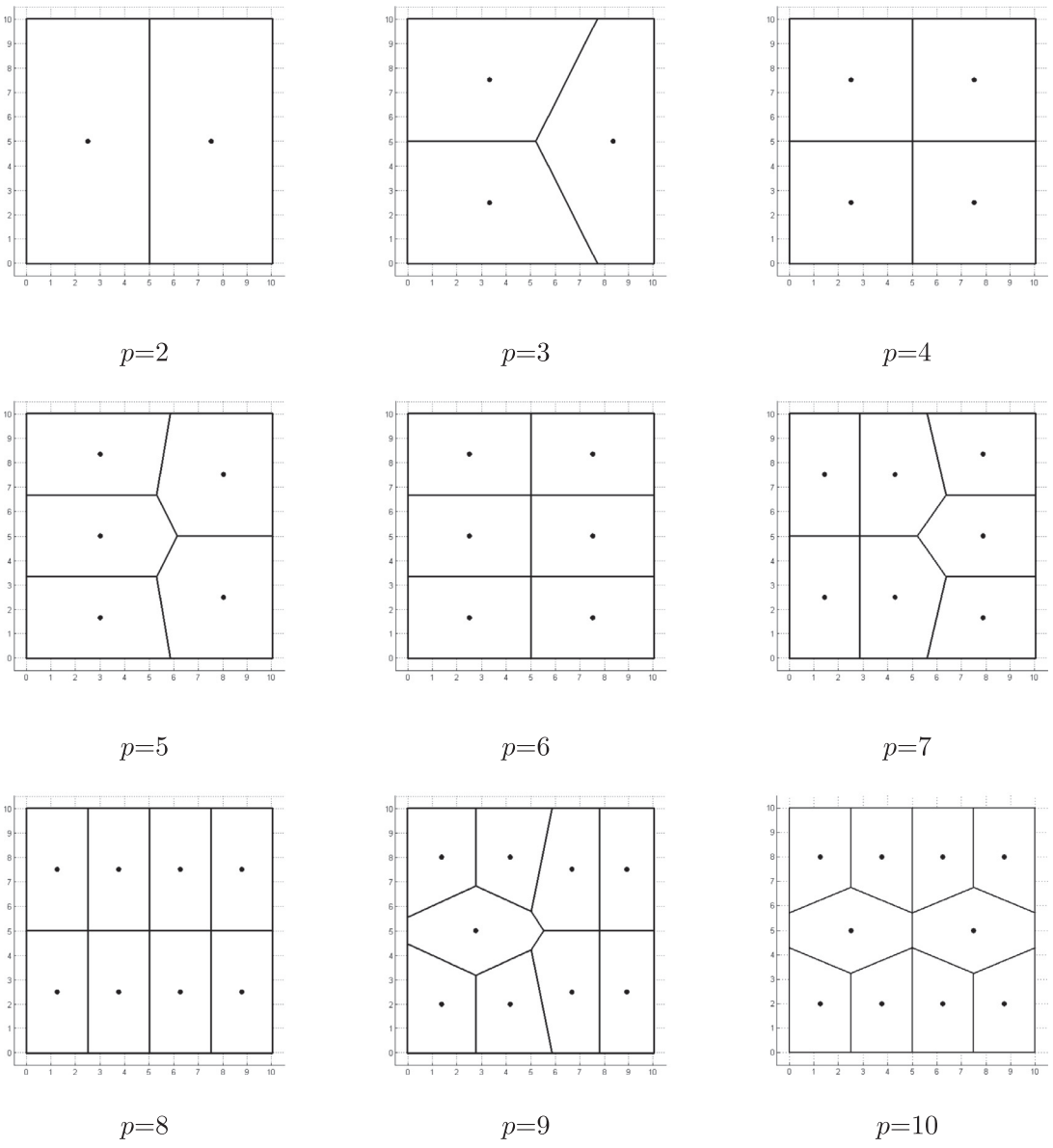

Fig. 7. Network configuration obtained by the algorithm proposed by Carlsson and Jia (2013).

Table 5
Results for solving the problem by the algorithm proposed by Carlsson and Jia (2013) with $\alpha = 0.4$ and $C = 10$.

p	$\delta = 30$			$\delta = 50$			$\delta = 70$		
	Total Cost	Gap with		Total Cost	Gap with		Total Cost	Gap with	
	C&J	IWA	PSO	C&J	IWA	PSO	C&J	IWA	PSO
2	13451.41	0.46	0.47	36192.17	0.47	0.48	69713.42	0.48	0.49
3	11690.49	0.89	0.93	31300.73	0.93	0.96	60126.18	0.95	0.98
4	10296.37	0.65	0.73	27428.16	0.68	0.76	52535.96	0.70	0.78
5	9841.85	1.37	1.38	26165.61	1.43	1.44	50061.35	1.46	1.48
6	9329.25	0.83	0.66	24741.74	0.87	0.89	47270.56	0.89	0.86
7	8925.37	0.76	0.79	23619.83	0.80	0.82	45071.62	0.82	1.10
8	8898.16	4.86	5.05	23544.25	5.11	5.12	44923.48	5.26	5.24
9	8517.20	4.29	4.28	22486.03	4.52	4.50	42849.38	4.66	4.62
10	8142.81	2.01	1.99	21446.05	2.12	1.93	40811.02	2.19	2.08
Avg.	9899.21	1.79	1.81	26324.95	1.88	1.88	50373.66	1.93	1.96

Table 6
Results for solving the problem by the algorithm proposed by Carlsson and Jia (2013) with $\alpha = 0.4$ and $\delta = 50$.

p	$C = 7$			$C = 10$			$C = 13$		
	Total Cost	Gap with		Total Cost	Gap with		Total Cost	Gap with	
	C&J	IWA	PSO	C&J	IWA	PSO	C&J	IWA	PSO
2	49975.75	0.49	0.50	36192.17	0.47	0.48	28770.26	0.46	0.47
3	42987.97	0.97	1.00	31300.73	0.93	0.96	25007.60	0.89	0.92
4	37455.74	0.71	0.80	27428.16	0.68	0.76	22028.71	0.65	0.73
5	35652.08	1.50	1.29	26165.61	1.43	1.44	21057.51	1.36	1.17
6	33617.98	0.91	0.74	24741.74	0.87	0.89	19962.23	0.83	0.84
7	32015.25	0.84	0.86	23619.83	0.80	0.82	19099.22	0.76	0.75
8	31907.28	5.41	5.33	23544.25	5.11	5.12	19041.08	4.85	4.87
9	30395.55	4.79	4.79	22486.03	4.52	4.50	18227.07	4.28	4.26
10	28909.87	2.25	2.17	21446.05	2.12	1.93	17427.09	2.01	1.96
Avg.	35879.72	1.99	1.94	26324.95	1.88	1.88	21180.09	1.79	1.77

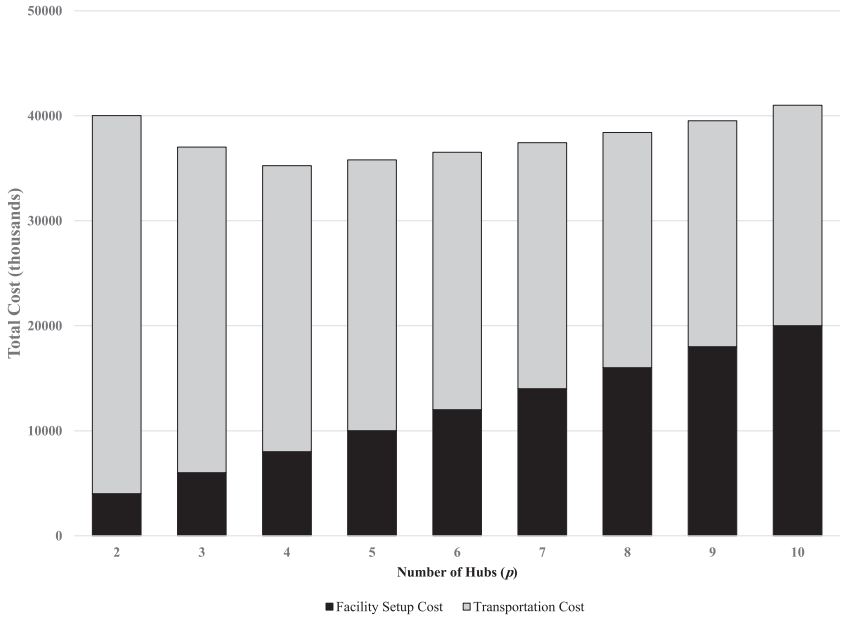

Fig. 8. Total cost change as function of the number of installed hubs p.

As in the previous cases, one can observe from Table 6 that the proposed algorithms show a better performance than the Carlsson and Jia's algorithm.

It should also be noted that, unlike the results reported in Table 4, the average gap does not vary significantly under different values of the demand points density (δ) and the vehicle capacity (C) as shown in Tables 5 and 6, respectively.

5.5. Optimal number of hubs

As we noted in the Section 3, the proposed model for the CAHLRP assumes that the number of hubs is given as an input parameter and hence, the proposed model and the solution heuristics do not determine the optimal number of hubs. In this part of our computational experiments, we show that one can easily use the proposed heuristics to determine the optimal number of hubs by incorporating the fixed costs for opening hubs into the analysis. For doing so, we set the fixed cost for opening a hub as 2 million dollars, which is equal for all hubs. We then solved the problem with different values of p ranging from 2 to 10 and obtained the total system-wide cost as the sum of the transportation and fixed facility setup costs. Fig. 8 illustrates the plots for the total system-wide cost and its components (i.e., the transportation and fixed hub installation costs) for varying numbers of installed hubs with $\alpha = 0.4$, $\delta = 50$, and $C = 10$.

As can be seen from Fig. 8, the transportation cost (including the ANC and the BNC) decreases as the number of installed hubs gets larger. In contrast, the facility setup cost increases as the number of hubs increases (proportional to the number of hubs). Note that the total cost reaches its minimum at $p = 4$. Therefore, the optimal number of hubs, assuming a fixed facility setup cost of 2 million dollars, is $p = 4$.

5.6. Alternative service region shapes

The proposed model and solution algorithms are applicable to any service region with a convex polygon shape and there is no limitation on the size of the polygon or the number of its sides. To show this, we conduct an additional set of experiments with a regular hexagonal service region. As in the square case, we assume that the total area of this hexagonal region is 100 km^2. Fig. 9 illustrates the resulting network configurations for different numbers of installed hubs with a hexagonal service region.

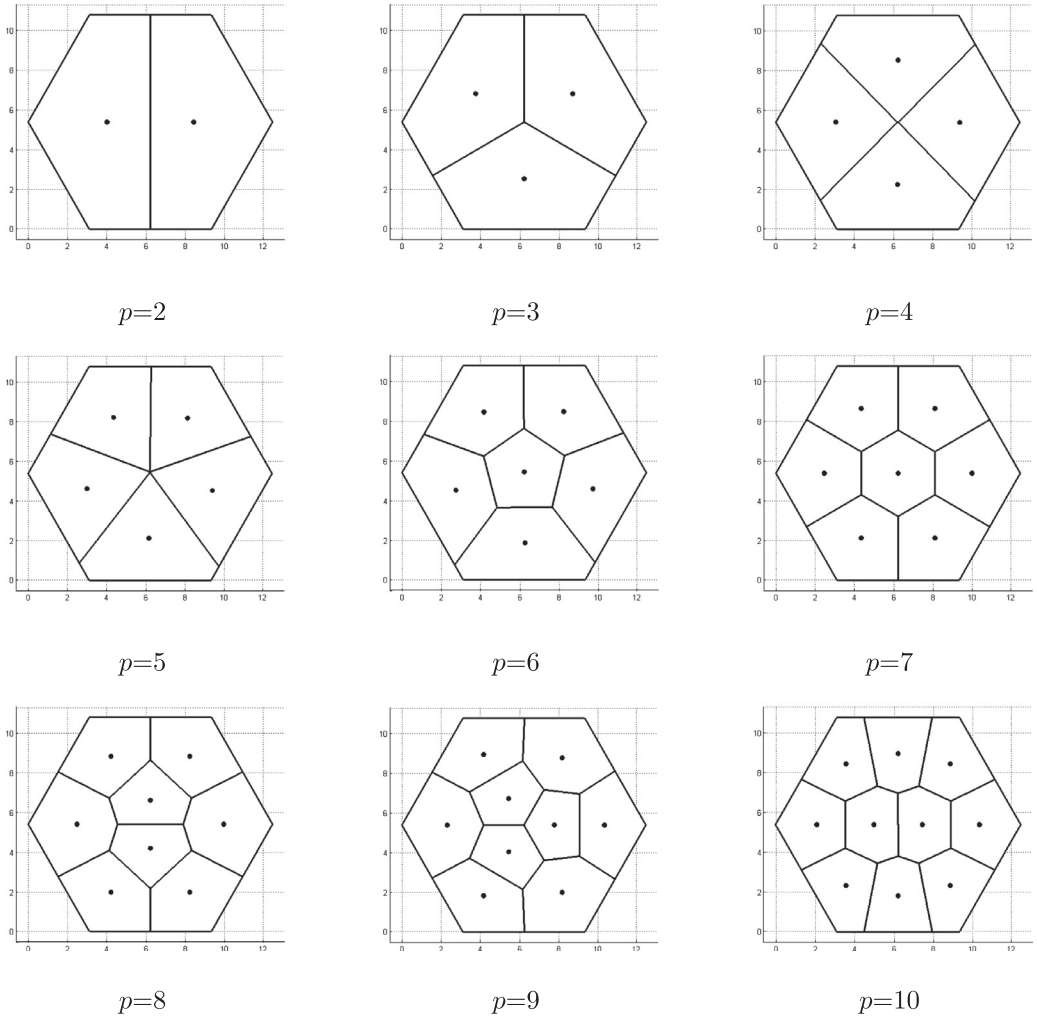

Fig. 9. Network configuration with different values of p for hexagonal service region ($\alpha = 0.4$).

6. Conclusions

This paper considered a planar hub location-routing problem where the market demand was modeled as a uniform density function and the distances were measured using the L_2 norm. Continuous approximation (CA) technique was used for modeling the problem with the aim of simultaneously deciding on the location of hubs and the allocation of service region to these hubs in such a way that the approximate total transportation cost, including local pickup and delivery cost, as well as line-haul inter-hub transportation cost is minimized. To solve the problem, two solution algorithms were proposed: an iterative Weiszfeld-type algorithm (IWA) and a particle swarm optimization (PSO) metaheuristic algorithm.

Extensive computational experiments were performed to evaluate the proposed solution algorithms. The results confirm the efficiency of the proposed solution algorithms in terms of their ability to generate quick and high quality solutions. The proposed solution algorithms were also compared with an adapted algorithm from the literature and it was shown that both of the proposed algorithms outperform the existing algorithm.

We also studied the influence of different input factors, such as the inter-hub transportation discount factor, demand point density, and vehicle capacity on the total system-wide cost. To show that the proposed solution methods can be applied to service regions of different shapes and sizes, we conducted another set of experiments with a hexagonal service region and presented the results.

Future research can be conducted in several directions. One might wish to try different density functions, rather than a uniform function, for modeling the market demand. Moreover, other distance metrics such as the rectilinear (or L_1) distance can be used, which might be more interesting in some situations like city logistics. Finally, some simplifying assumptions, such as having a complete network between hub facilities or flow-independent economies of scale only on inter-hub connections, can be relaxed in order to make the proposed model suitable for application to more realistic settings.

Acknowledgment

The authors sincerely thank the two anonymous referees for their valuable and constructive comments that helped us improve the quality and presentation of the paper.

Appendix A. The average distance from a point within a convex polygon

In this appendix, we first calculate the average distance from uniformly distributed points within a triangle to one of its vertices based on the method used in Mathpages[dot]com (2014). Then, using the formula obtained for a triangle, we derive a closed-form formula for calculating the average distance from a point within a convex polygon to evenly scattered points over that polygon.

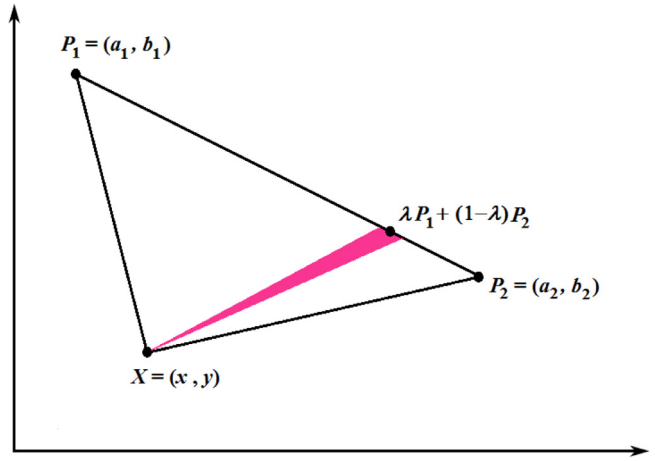

Fig. A.10. A general triangle and a shaded narrow sector inside it.

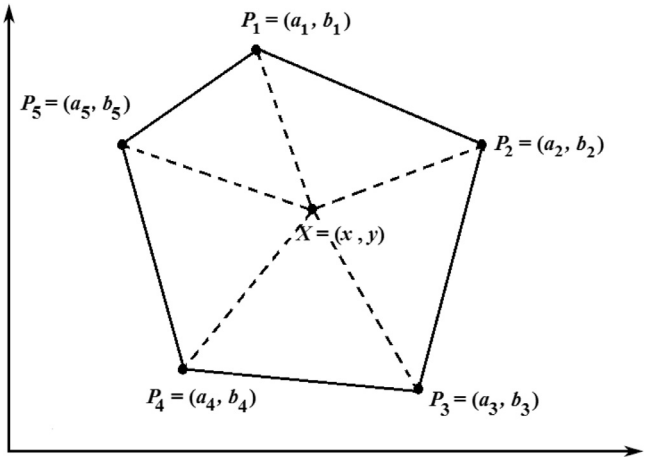

Fig. A.11. A typical polygon as union of triangles.

Fig. A.10 illustrates a general triangle with the coordinates of its vertices.

If we approximate the shaded region in the above figure as a narrow sector from a circle centered at X and with the radius $\|X - (\lambda P_1 + (1-\lambda)P_2)\|$, then the average distance from point X to all points evenly distributed within this region is calculated as $\frac{2}{3}\|X - (\lambda P_1 + (1-\lambda)P_2)\|$. This is because the average distance from the center of a circle of radius r to its interior is $\frac{2}{3}r$. Consequently, we can derive the formula for the average distance from a vertex to the points within a triangle as follows:

$$\bar{\rho}_{tri} = \frac{2}{3}\int_0^1 \|X - (\lambda P_1 + (1-\lambda)P_2)\| d\lambda \tag{A.1}$$

Proposition 1. *A closed-form for calculating $\bar{\rho}_{tri}$ is:*

$$\bar{\rho}_{tri} = \frac{\|P_2 - P_1\|}{6}\left(\theta(1+\phi^2) + \frac{1}{2}(1-\theta^2)(1-\phi^2)\ln\left(\frac{\theta-1}{\theta+1}\right)\right) \tag{A.2}$$

in which

$$\theta = \frac{\|X - P_2\| + \|X - P_1\|}{\|P_2 - P_1\|},$$

$$\phi = \frac{\|X - P_2\| - \|X - P_1\|}{\|P_2 - P_1\|}.$$

Proof. Let I be defined as the following definite integral:

$$I = \int_0^1 \|X - (\lambda P_1 + (1-\lambda)P_2)\| \, d\lambda = \int_0^1 \sqrt{(x - \lambda a_1 - (1-\lambda)a_2))^2 + (y - \lambda b_1 - (1-\lambda)b_2)^2} \, d\lambda$$

$$= \int_0^1 \sqrt{((a_2 - a_1)^2 + (b_2 - b_1)^2)\lambda^2 + 2((x - a_2)(a_2 - a_1) + (y - b_2)(b_2 - b_1))\lambda + (x - a_2)^2 + (y - b_2)^2} \, d\lambda$$

$$= \int_0^1 \sqrt{\|P_2 - P_1\|^2\lambda^2 + 2\langle X - P_2, P_2 - P_1\rangle\lambda + \|X - P_2\|^2} \, d\lambda$$

$$= \int_0^1 \sqrt{\|P_2 - P_1\|^2\lambda^2 + (\|X - P_1\|^2 - \|P_2 - P_1\|^2 - \|X - P_2\|^2)\lambda + \|X - P_2\|^2} \, d\lambda$$

From calculus, we know that:

$$\int \sqrt{ax^2 + bx + c} \, dx = \frac{b + 4ax}{4a}\sqrt{ax^2 + bx + c} + \frac{4ac - b^2}{8a^{3/2}} \ln\left|2ax + b + 2\sqrt{a(ax^2 + bx + c)}\right| + C$$

Replacing the parameters a, b, and c in the above formula and doing the required simplifications, the solution to the definite integral (I) can be expressed as:

$$I = \frac{\|P_2 - P_1\|}{4}\left(\theta(1+\phi^2) + \frac{1}{2}(1-\theta^2)(1-\phi^2)\ln\left(\frac{\theta-1}{\theta+1}\right)\right)$$

Hence, the average distance from a vertex of a triangle to the points evenly distributed within that triangle can be calculated as follows:

$$\bar{\rho}_{tri} = \frac{2}{3}\int_0^1 \|X - (\lambda P_1 + (1-\lambda)P_2)\| d\lambda$$

$$= \frac{\|P_2 - P_1\|}{6}\left(\theta(1+\phi^2) + \frac{1}{2}(1-\theta^2)(1-\phi^2)\ln\left(\frac{\theta-1}{\theta+1}\right)\right).$$

□

Now consider a polygon $\mathcal{V}$ of n sides formed by points (in clockwise order) $P_i, i = 1, \ldots, n$ and let X be a point inside this polygon from which we want to calculate the average distance to points inside the polygon, i.e., $\bar{\rho}(\mathcal{V}, X)$. Fig. A.11 depicts such a polygon with 5 sides. It can be easily shown that the average distance from point X to points within this polygon equals the weighted sum of the average distance from X to the points within the triangles formed by $\{X, P_i, P_{i+1}\}, i = 1, \ldots, n$ with $P_{n+1} = P_1$. The weight associated with the average distance for each triangle is the proportion between the area of that triangle and the area of the whole polygon. Based on the definition of matrix determinants, we can calculate the area of the triangle formed by $\{X, P_i, P_{i+1}\}$ as $\frac{1}{2}\det(P_{i+1} - P_i, P_i - X)$ and the area of the whole polygon as $\frac{1}{2}\sum_{i=1}^{n}\det(P_{i+1}, P_i)$, where $\det(P_{i+1}, P_i)$ is the determinant formed by vectors P_{i+1} and P_i,

$$\det(P_{i+1}, P_i) = \begin{vmatrix} a_{i+1} & a_i \\ b_{i+1} & b_i \end{vmatrix}$$

Hence, $\bar{\rho}(\mathcal{V}, X)$ can be calculated by using the following closed-form expression:

$$\bar{\rho}(\mathcal{V}, X) = \frac{\sum_{i=1}^{n} \bar{\rho}_{tri(i)} \det(P_{i+1} - P_i, P_i - X)}{\sum_{i=1}^{n} \det(P_{i+1}, P_i)}$$

$$= \frac{\sum_{i=1}^{n} \|P_{i+1} - P_i\| \left(\theta_i(1+\phi_i^2) + \frac{1}{2}(1-\theta_i^2)(1-\phi_i^2)\ln(\frac{\theta_i - 1}{\theta_i + 1})\right) \det(P_{i+1} - P_i, P_i - X)}{6\sum_{i=1}^{n} \det(P_{i+1}, P_i)} \quad \text{(A.3)}$$

in which

$$\theta_i = \frac{\|X - P_{i+1}\| + \|X - P_i\|}{\|P_{i+1} - P_i\|},$$

$$\phi_i = \frac{\|X - P_{i+1}\| - \|X - P_i\|}{\|P_{i+1} - P_i\|}.$$

Having derived a closed-form expression for the average distance from a point inside a convex polygon to all points evenly distributed within that polygon, $\bar{\rho}(\mathcal{V}, X)$, one can easily minimize this distance by using any convex optimization tool to obtain the Fermat-Weber point of that polygon.

References

Ai, T.J., Kachitvichyanukul, V., 2009. A particle swarm optimization for the vehicle routing problem with simultaneous pickup and delivery. Comput. Oper. Res. 36 (5), 1693–1702.

Aurenhammer, F., 1991. Voronoi diagrams-a survey of a fundamental geometric data structure. ACM Comput. Surv. 23 (3), 345–405.

Aykin, T., 1995. The hub location and routing problem. Eur. J. Oper. Res. 83, 200–219.

Bailey, A., Ornbuki-Berrnan, B., Asobiela, S., 2013. Discrete PSO for the uncapacitated single allocation hub location problem. In: Computational Intelligence In Production And Logistics Systems (CIPLS), 2013 IEEE Workshop on, pp. 92–98.

Banks, A., Vincent, J., Anyakoha, C., 2007. A review of particle swarm optimization. part I: background and development. Nat. Comput. 6 (4), 467–484.

Banks, A., Vincent, J., Anyakoha, C., 2008. A review of particle swarm optimization. Part II: hybridisation, combinatorial, multicriteria and constrained optimization, and indicative applications. Nat. Comput. 7 (1), 109–124.

Beardwood, J., Halton, J.H., Hammersley, J.M., 1959. The shortest path through many points. Math. Proc. Cambridge Philos. Soc. 55 (4), 299–327.

Cachon, G.P., 2014. Retail store density and the cost of greenhouse gas emissions. Manag. Sci. 60 (8), 1907–1925.

de Camargo, R.S., de Miranda, G., Løkketangen, A., 2013. A new formulation and an exact approach for the many-to-many hub location-routing problem. Appl. Math. Model. 37 (12–13), 7465–7480.

Campbell, J.F., 1990. Freight consolidation and routing with transportation economies of scale. Transp. Res. Part B 24 (5), 345–361.

Campbell, J.F., 1990. Locating transportation terminals to serve an expanding demand. Transp. Res. Part B 24 (3), 173–192.

Campbell, J.F., 2013. A continuous approximation model for time definite many-to–many transportation. Transp. Res. Part B 54, 100–110.

Campbell, J.F., O'Kelly, M.E., 2012. Twenty-five years of hub location research. Transp. Sci. 46 (2), 153–169.

Carlsson, J.C., Jia, F., 2013. Euclidean hub-and-spoke networks. Oper. Res. 61 (6), 1360–1382.

Çetiner, S., Sepil, C., Süral, H., 2010. Hubbing and routing in postal delivery systems. Ann. Oper. Res. 181 (1), 109–124.

Christofides, N., Eilon, S., 1969. Expected distances in distribution problems. Oper. Res. Q. 20, 437–443.

Crainic, T.G., Laporte, G., 1997. Planning models for freight transportation. Eur. J. Oper. Res. 97 (3), 409–438.

Daganzo, C.F., 1984. The distance traveled to visit *N* points with a maximum of c stops per vehicle: an analytic model and an application. Transp. Sci. 18 (4), 331–350.

Daganzo, C.F., 1984. The length of tours in zones of different shapes. Transp. Res. Part B 18 (2), 135–145.

Daganzo, C.F., 1987. The break-bulk role of terminals in many-to-many logistic networks. Oper. Res. 35 (4), 543–555.

Daganzo, C.F., 2005. Logistics Systems Analysis, 4 ed. Springer, Heidelberg, Germany.

Eilon, S., Watson-Gandy, C.D.T., Christofides, N., 1971. Distribution management: Mathematical modelling and practical analysis. Hafner, New York.

Erlenkotter, D., 1989. The general optimal market area model. Ann. Oper. Res. 18 (1), 43–70.

Francis, P., Smilowitz, K., 2006. Modeling techniques for periodic vehicle routing problems. Transp. Res. Part B 40 (10), 872–884.

Francis, R.L., McGinnis, L.F., White, J.A., 1992. Facility Layout and Location: An Analytical Approach. Pearson College Division.

Geoffrion, A.M., 1976. The purpose of mathematical programming is insight, not numbers. Interfaces 7 (1), 81–92.

Hall, R.W., 1986. Discrete models/continuous models. Omega 14 (3), 213–220.

Herceg, M., Kvasnica, M., Jones, C., Morari, M., 2013. Multi-parametric toolbox 3.0. In: Proc. of the European Control Conference. Zrich, Switzerland, pp. 502–510. http://control.ee.ethz.ch/~mpt

Jabali, O., Gendreau, M., Laporte, G., 2012. A continuous approximation model for the fleet composition problem. Transp. Res. Part B 46, 1591–1606.

Kennedy, J., Eberhart, R.R., 1995. Particle swarm optimization. In: Proceedings of the IEEE International Conference on Neural Networks. Piscataway, NJ, pp. 1942–1948.

Langevin, A., Mbaraga, P., Campbell, J.F., 1996. Continuous approximation models in freight distribution: an overview. Transp. Res. Part B 30 (3), 163–188.

Laporte, G., 1992. The vehicle routing problem: an overview of exact and approximate algorithms. Eur. J. Oper. Res. 59 (3), 345–358.

Liu, Y., Wu, X., Hao, F., 2012. A new chance variance optimization criterion for portfolio selection in uncertain decision systems. Expert Syst. Appl. 39 (7), 6514–6526.

Marinakis, Y., Marinaki, M., 2010. A hybrid genetic particle swarm optimization algorithm for the vehicle routing problem. Expert Syst. Appl. 37 (2), 1446–1455.

Mathpages[dot]com, 2014. Mean distance from vertex to interior of plane figures. http://www.mathpages.com/home/kmath283/kmath283.htm.

Miehle, W., 1958. Link-length minimization in networks. Oper. Res. 6 (2), 232–243.

Murat, A., Verter, V., Laporte, G., 2010. A continuous analysis framework for the solution of location allocation problems with dense demand. Comput. Oper. Res. 37 (1), 123–136.

Nagy, G., Salhi, S., 1998. The many-to-many location-routing problem. TOP 6 (2), 261–275.

Newell, G.F., 1973. Scheduling, location, transportation, and continuum mechanics: some simple approximations to optimization problems. SIAM J. Appl. Math. 25 (3), 346–360.

O'Kelly, M.E., Miller, H.J., 1994. The hub network design problem: a review and synthesis. J. Transp. Geogr. 2 (1), 31–40.

Pedrycz, W., Park, B., Pizzi, N., 2009. Identifying core sets of discriminatory features using particle swarm optimization. Expert Syst. Appl. 36 (3, Part 1), 4610–4616.

Pulido, R., Muñoz, J., Gazmuri, P., 2015. A continuous approximation model for locating warehouses and designing physical and timely distribution strategies for home delivery. EURO J. Transp. Logist. 4 (4), 399–419.

Radó, F., 1988. The euclidean multifacility location problem. Oper. Res. 36 (3), 485–492.

Rieck, J., Ehrenberg, C., Zimmermann, J., 2014. Many-to-many location-routing with inter-hub transport and multi-commodity pickup-and-delivery. Eur. J. Oper. Res. 236 (3), 863–878.

Rodríguez-Martín, I., Salazar-González, J.-J., Yaman, H., 2014. A branch-and-cut algorithm for the hub location and routing problem. Comput. Oper. Res. 50 (0), 161–174.

Saberi, M., Mahmassani, H.S., 2013. Modeling the airline hub location and optimal market problems with continuous approximation techniques. J. Transp. Geogr. 30, 68–76.

Sevkli, M., Guner, A.R., 2006. A Continuous Particle Swarm Optimization Algorithm for Uncapacitated Facility Location Problem. Springer Berlin Heidelberg, Berlin, Heidelberg, pp. 316–323.

Sha, D., Hsu, C.-Y., 2008. A new particle swarm optimization for the open shop scheduling problem. Comput. Oper. Res. 35 (10), 3243–3261.

Shen, Z.-J.M., Qi, L., 2007. Incorporating inventory and routing costs in strategic location models. Eur. J. Oper. Res. 179 (2), 372–389.

Smilowitz, K.M., Daganzo, C.R., 2007. Continuum approximation techniques for the design of integrated package distribution systems. Networks 50, 183–196.

Suzuki, A., Drezner, Z., 1997. On the airline hub problem: the continuous model. J. Oper. Res. Soc.Jpn. 40 (1), 62–74.

Von Hohenbalken, B., West, D.S., 1984. Manhattan versus euclid: market areas computed and compared. Reg. Sci. Urban Econ. 14 (1), 19–35.

Weiszfeld, E., 1973. Sur le point pour lequel la somme des distances de *N* points donnés est minimum. Tôhoku Math. J. 43, 355–387.

Xie, W., Ouyang, Y., 2015. Optimal layout of transshipment facility locations on an infinite homogeneous plane. Transp. Res. Part B 75, 74–88.

Yang, K., Liu, Y., Yang, G., 2013. An improved hybrid particle swarm optimization algorithm for fuzzy p-hub center problem. Comput. Ind. Eng. 64 (1), 133–142.

Zäpfel, G., Wasner, M., 2002. Planning and optimization of hub-and-spoke transportation networks of cooperative third-party logistics providers. Int. J. Prod. Econ. 78 (2), 207–220.

Zhao, F., Tang, J., Wang, J., Jonrinaldi, 2014. An improved particle swarm optimization with decline disturbance index (DDPSO) for multi-objective job-shop scheduling problem. Comput. Oper. Res. 45, 38–50.